



One-pot synthesis of green-emitting gold nanoclusters as a fluorescent probe for determination of 4-nitrophenol

Yu Li^{1,2} · Qiu-Lin Wen¹ · An-Yong Liu¹ · Yunfei Long³ · Peng Liu¹ · Jian Ling¹ · Zhong-Tao Ding¹ · Qiu-E Cao¹

Received: 31 July 2019 / Accepted: 17 December 2019 / Published online: 8 January 2020
© Springer-Verlag GmbH Austria, part of Springer Nature 2020

Abstract

A hydrothermal method was applied to the synthesis of green-emitting gold nanoclusters (Au NCs) which are shown to be viable fluorescent probes for 4-nitrophenol (4-NP). The Au NCs were prepared by using thiol- β -cyclodextrin as a template. Under 365 nm excitation, their green fluorescence has a peak at 502 nm, with a narrow emission bandwidth of only 30 nm. The fluorescence and composition of the Au NCs were characterized and the mechanism of the nanocluster formation is discussed. Due to host-guest recognition of β -cyclodextrin and 4-NP, fluorescence is quenched. The probe can selectively recognize 4-NP among other nitrophenols. A fluorometric and colorimetric assay was developed for 4-NP that works in the 0.1 to 100 μ M concentration range and has a detection limit of 90 nM (at 3σ).

Keywords Metal nanoclusters · Thiol- β -cyclodextrin · Host-guest recognition · Fluorometry · Colorimetry

Introduction

Fluorescent noble metal nanoclusters are a special type of ultra-small nanoparticles (< 2 nm core diameter) protected by stabilizer agents and exhibiting intense fluorescence. These nanoclusters induce distinctive quantum confinement effects, which result in a discrete electronic structure and molecular-like properties, such as the highest occupied molecular orbital and lowest unoccupied molecular orbital (HOMO-

LUMO) electronic transition, photoluminescence, intrinsic magnetism et al. [1]. The emission wavelength of nanoclusters is found to be strongly dependent on the number of metal atoms in core [2, 3]. Fluorescent noble metal nanoclusters, especially gold nanoclusters (Au NCs) were served as a novel optical sensor for environmental monitoring due to their fluorescence stability, biocompatibility and wide emission spectrum ranges [4]. It has become a promising material due to their fascinating performance, such as being eco-friendly and having high colloidal stability, superior catalytic activity, unusual photophysical properties, and good biocompatibility [5], which facilitates applications in bioimaging [6], catalysis [7], biochemical sensing [8, 9], environmental monitoring and the determination of heavy metal ions [10, 11] and inorganic anions [12].

There are many efforts have been devoted to synthesizing Au NCs. In the past decades, DNA [8, 13], peptide [14], natural polymeric compound [15, 16], small molecule [17], protein [18] were applied as templates to prepare Au NCs emitted from blue to near-infrared regions. However, most of fluorescent Au NCs reported are red-emission (around 650 nm) fluorescent NCs, green-emission Au NCs were less reported and applied for analytical purposes. For example, Jiang et al. reported a method for determination of GSH activity by using cytidine stabilized Au NCs emitted at 505 nm [19]. Bain et al. have prepared photostable, water-soluble and highly green-emission fluorescent Au NCs by ligand

Electronic supplementary material The online version of this article (<https://doi.org/10.1007/s00604-019-4090-5>) contains supplementary material, which is available to authorized users.

✉ Jian Ling
lingjian@ynu.edu.cn

✉ Qiu-E Cao
qecao@ynu.edu.cn

¹ Functional Molecules Analysis and Biotransformation Key Laboratory of Universities in Yunnan Province, School of Chemical Science and Technology, Yunnan University, Kunming 650091, China

² Xi'an Institute for Innovative Earth Environment Research, Institute of Earth Environment, Chinese Academy of Sciences, Xi'an 710061, China

³ School of Chemistry and Chemical Engineering, Hunan University of Science and Technology, Xiangtan 411201, Hunan, China

exchange and core etching technique for determination of Pb^{2+} [20]. Kawasaki et al. reported a pH-dependent synthesis of Au NCs (Au_{13}) with green fluorescent emission using porcine pepsin [21]. Thus, studies on the preparation of a wide range color of fluorescence Au NCs by a number of templates for analytical application is still attracted much attention of researchers.

Cyclodextrins, especially β -cyclodextrin (β -CD), as macrocyclic molecules, which are toroidal in shape with a hydrophobic inner cavity and a hydrophilic exterior [22]. The interesting characteristics can enable them to bind a wide variety of hydrophobic guest molecules to form stable host–guest complex in their hydrophobic cavity, which has stimulated particular attention in fluorescence probing and in biosensing platforms of organic molecules [23]. Considerable research efforts have been devoted to synthesis metal nanoclusters (Au, Ag, Cu) by introducing CD [24, 25]. Grafted CD was also used to have synthesized highly water-soluble fluorescence nanoclusters as a multifunctional nanoprobe for biological applications [26].

We developed a new strategy for the synthesis of a new green emission gold nanoclusters by introducing thiol- β -cyclodextrin (thiol-CD) as a template and reduction reagent. The thiol- β -cyclodextrin stabilized gold nanoclusters (thiol-CD-Au NCs) has a green fluorescence emission at 502 nm with very narrow emission bandwidth of 30 nm. Due to host-guest recognition of β -cyclodextrin with 4-nitrophenol, the thiol-CD-Au NCs exhibit an efficient ability of recognition of 4-nitrophenol from other nitrophenols. The method can be used to quantify 4-nitrophenol in the range from 0.1 to 100 μM with detection limits of 0.09 (3σ).

Nitrophenol is widely applied in the production of fine chemicals and pharmaceuticals [27], which includes three isomers, 2-nitrophenol (2-NP), 3-nitrophenol (3-NP) and 4-nitrophenol (4-NP), respectively. However, that is proved that 4-NP is carcinogenic, mutagenic and has cyto- and embryonic toxicity even at low concentration [28, 29]. Therefore, it is of significance to develop simple and effective methods for trace 4-NP. Up to now, various techniques have been developed to determine 4-NP, including flow injection technique [30], electrochemical sensor [31, 32], fluorescence sensors [33, 34], spectrophotometry [35, 36] and capillary electrophoresis [37]. The present method proposed here is simple and rapid with sensitivity and selectivity comparable to these assays.

Experimental section

Chemicals and instruments

Hydrogen tetrachloroaurate hydrate ($\text{HAuCl}_4 \cdot 4\text{H}_2\text{O}$, 99.9%) was obtained from Sinopharm Chemical Reagent Co., Ltd. (<https://www.reagent.com.cn/>). mono-

(6-mercapto-6-deoxy)- β -cyclodextrin (thiol-CD, 98%) was purchased from Shandong Binzhou Zhiyuan Bio-Technology Co., Ltd. (<http://www.bzzysw.com/>). Sodium hydroxide (NaOH, AR), N, N-dimethylformamide (DMF, AR) were purchased from Guangdong Guanghua Sci-Tech Co., Ltd. (<http://www.ghotech.com/>). 2-nitrophenol and 4-nitrophenol (analytical grade) were purchased from Shanghai Titan Scientific Co., Ltd. (<http://www.titansci.com/index.action>). Ultrapure water (Milli-Q) with a resistivity of 18.25 $\text{M}\Omega$ was used as the general solvent throughout the study. All other chemicals were of analytical grade and used without further modification.

Fluorescence spectra were recorded with an F-7000 spectrophotometer (Hitachi, Japan). Absorption spectra were recorded using a UV-2550 spectrophotometer (Shimadzu, Japan). Transmission electron microscopic (TEM) images were acquired on a JEM-2100TEM (JEOL, Japan) with an accelerating voltage of 200 KV. The X-ray photoelectron spectroscopic (XPS) data were collected on a *K-Alpha*⁺ X-ray photoelectron spectrometer (Thermo Fisher Scientific) with an Al $K\alpha = 1486.6$ eV excitation source. Fourier-transform infrared (FTIR) spectroscopy analyses were performed on a Nicolet iS10 (Thermo Fisher Scientific) using KBr pellets. Matrix-assisted laser desorption ionization-time-of-flight (MALDI-TOF) mass spectrometry was carried out on an Ultrafine Xtreme MALDI-TOF (Bruker Daltonics Autoflex II TOF/TOF).

Synthesis of thiolated cyclodextrin-gold nanoclusters (thiol-CD-Au NCs)

Synthesis of thiol-CD-Au NCs was carried out hydrothermally using mono-(6-mercapto-6-deoxy)- β -cyclodextrin (thiol-CD) and hydrogen tetrachloroaurate hydrate ($\text{HAuCl}_4 \cdot 4\text{H}_2\text{O}$). All glassware was immersed in Aqua Regia solution ($\text{HCl}/\text{HNO}_3 = 3:1$, v/v) for several hours, then washed thoroughly by ethanol and ultrapure water prior to use. The typical procedure for the synthesis of thiol-CD stabilized Au NCs is presented as follows: After heating an aqueous solution of $\text{HAuCl}_4 \cdot 4\text{H}_2\text{O}$ (1 mM, 5.0 mL) in 50 mL round bottom flask at 90 °C for 10 min, thiol-CD (dissolved in the DMF, 10 mM, 2 mL) was added under continuous heating and vigorous stirring keeping the molar ratio between AuCl_4^- and thiol-CD at 1:4. NaOH solution (1.5 mL, 2 M) was quickly added into the mixture after 5 min. Yellow deposition can be seen in the round bottom flask after 4 h, indicating the formation of luminescent thiol-CD-Au NCs. The product was centrifuged at 8000 rpm and washed by water for three times. Finally, a certain amount of DMF solution was added to dissolve thiol-CD-Au NCs to prepare a stock solution for use.

Procedure for determination of 4-nitrophenol

The assay was performed in a 1.5 mL centrifuge tube at room temperature. Typically, various volumes of 4-nitrophenol stock solutions were added to 300 μL thiol-CD-Au NCs solutions and diluted to 1.0 mL with DMF. After mixing well for 30 s, the solutions were characterized directly by UV-vis spectrophotometer or fluorescence spectrophotometer.

Result and discussion

Characterization of thiol-CD-Au NCs

The fluorescence and adsorption feature of the gold nanoclusters (Au NCs) are measured and shown in Fig. 1. The Au NCs has a very narrow green-emission peak at 502 nm (with a bandwidth of 30 nm) and an excitation peak at 365 nm. As the emission wavelength of Au NCs is found to be strongly dependent on the number of metal atoms in core [20], the Au NCs is smaller than the reported red-emission Au NCs stabilized by GSH and proteins [38, 39]. The large Stokes shift in the excitation at 365 nm and the emission maximum is seen at 502 nm, which may be due to charge transfer between the ligand metals [40]. We use time-resolved fluorescence to measure the luminescence lifetime of the thiol-CD-Au NCs. Under 370 nm excitation, 502 nm-emitting Au NCs has fitted average luminescence lifetime of 25.23 ± 1.18 ns. (Fig. S1).

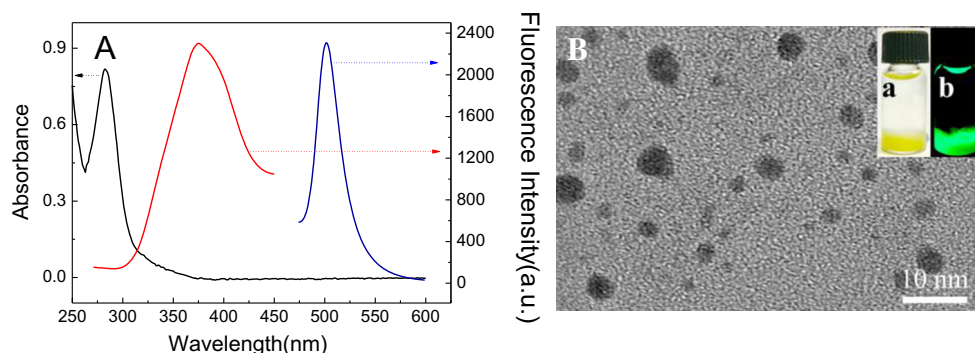
UV-vis absorption spectrum of Au NCs (Fig. 1a, the blank line) shows that the fluorescence is a typical emission from Au NCs and no Au nanoparticles produced in the NCs preparation process. However, there is an absorption peak at 283 nm which is attributed to the doping of sulfur elements along with the strong absorption band of nanoclusters structure. The shape and size of the NCs were observed by high-resolution TEM. As shown in Fig. 1b, the NCs is monodisperse with an average size of 3.5 ± 1 nm. The raw product of the Au NCs is yellow precipitate in aqueous solution and emitted intense green luminescence under UV light (Fig. 1b inset).

To identify the chemical elements of the Au NCs, X-ray photoelectric spectroscopy (XPS) is used to compare the chemical elements in thiol-CD and the thiol-CD-Au NCs (Fig. S2A-F). After formation of fluorescent thiol-CD-Au NCs, several peaks of Au 4f (83.68 and 84.37 eV), Au 4d (335 and 352 eV) appear (Fig. 2a). Furthermore, the Au 4f, O 1s, C 1s, S 2p peaks in the XPS spectra are deconvoluted to understand the change in chemical species before and after the formation of Au NCs. The thiol-CD-Au NCs shows a characteristic twin XPS peak between 80 and 90 eV, which is assigned as 4f of Au (Fig. 2b). The higher binding energies (84.37 and 88.00 eV) are assigned for Au^+ and the lower energies (83.68 and 87.30 eV) are arising from the presence of Au^0 . Therefore, the evidence indicates the coexistence of both Au^0 and Au^+ in the thiol-CD-Au NCs. Thiol-CD-Au NCs has a carbonyl group owing to the oxidation of hydroxyl groups by AuCl_4^- [25]. The deconvolution of C 1s spectra of thiol-CD (Supporting materials, Fig. S2D) and thiol-CD-Au NCs (Fig. 2c) also clearly indicate the appearance of the carbonyl groups in the Au NCs.

The higher binding energy around 163.52 eV is assigned for $2p_{1/2}$ which is arising from S – C bond present in the capping ligand itself (As shown in Fig. S2F). The shoulder peak around 162.23 eV is for $2p_{3/2}$, which is arising from Au – S covalent bond formation [20]. Therefore, these results clearly indicate that the hydroxyl groups in the cyclodextrin were oxidized and the thiol group was closely linked onto the Au NCs surface. In addition, the C, O, and S atoms contribute 67.51, 30.3, and 1.85 wt.% to the thiol-CD-Au NCs, respectively (in Electronic Supporting Material, Table S1).

The Fourier-transform infrared (FTIR) measurements are carried out to get more information about the thiol-CD-Au NCs and thiol-CD. The results provide more evidence for the role of thiol-CD as a reducing agent. As shown in Fig. 2d, the characteristics peak position of -OH shifted from 3398.14 cm^{-1} to 3418.99 cm^{-1} and two new peaks corresponding to the C=O stretching vibration and -COO- symmetrical stretching vibration of Au-COO⁻ appeared around 1606.75 cm^{-1} and 1362.97 cm^{-1} , respectively. The C-H stretching vibration of Au-C=O⁻ at 2718.57 cm^{-1} and

Fig. 1 **a** UV-vis absorption (black line) and fluorescence excitation (red line, $\lambda_{\text{ex}} = 365$) and emission (blue line, $\lambda_{\text{em}} = 502$) spectra of the thiol-CD-Au NCs. **b** TEM images and photographs of the thiol-CD-Au NCs under daylight (*a*) and the 365 nm of UV light (*b*)



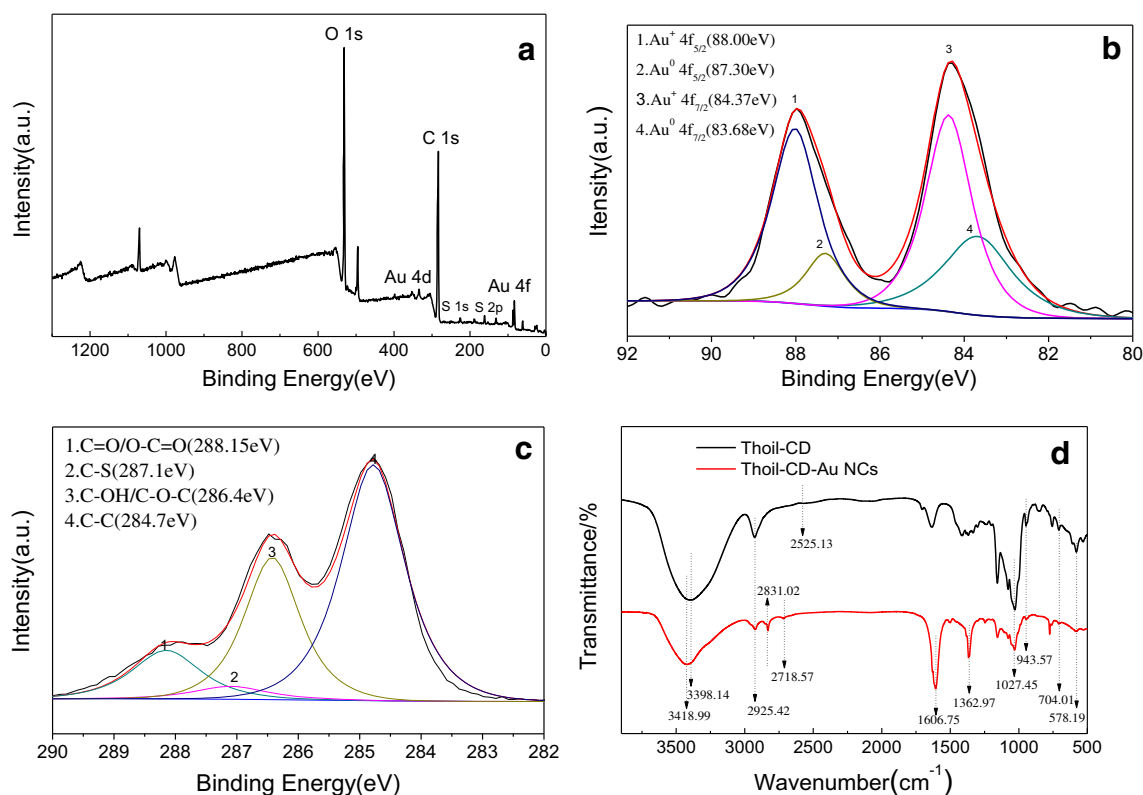


Fig. 2 **a** X-ray photoelectron spectra of thiol-CD-Au NCs. **b** The deconvolution of Au 4f spectra of thiol-CD-Au NCs. **c** The deconvolution of C1s spectra of thiol-CD-Au NCs. **d** FT-IR spectra of thiol-CD (black line) and thiol-CD-Au NCs (red line)

2831.02 cm^{-1} also appears. The results confirm the oxidation of thiol-CD in the Au NCs synthesis. The S-H bond vibration of thiol-CD at 2525.13 cm^{-1} is disappeared owing to the formation of a stable Au-S covalent bond after the formation of Au NCs. This clearly proves that thiol-CD were attached on the surface of Au NCs.

The matrix-assisted laser desorption/ionization time-of-flight mass spectrometry (MALDI-TOF MS) is also used to uncover more detailed information of thiol-CD-Au NCs. As shown in Electronic Supporting Material, Fig. S3 A and B, the mass spectral peak of thiol-CD is shifted from 1310.01 to 2219.64 Da after the formation of the thiol-CD-Au NCs. Although it is hard to know the structure of thiol-CD-Au NCs at atomically precise, the results indicate the formation of Au NCs that packaged in thiol-CD molecules.

Optimization of Au nanocluster synthesis condition

For the preparation of the green-emission thiol-CD-Au NCs, some experimental conditions, such as temperature, thiol-CD and NaOH concentration is critical. For example, if none of capping agents (thiol-CD) was added, black precipitation without fluorescence would appear in the bottom of the round-bottomed flask, if the reaction was placed a lower temperature, no fluorescent NCs was produced in more than 24 h. Only in the presence of an appropriate amount of HAuCl_4 ,

thiol-CD, NaOH and at the high reaction temperature, the green-emission Au NCs would be synthesized (Supporting materials, Fig. S4).

The molar ratios of HAuCl_4 and thiol-CD for Au NCs preparation was firstly studied. It can be seen in Supporting materials, Fig. S5 A and B, if the ratio of HAuCl_4 to thiol-CD is between 1:3 and 1:8, a fluorescence peak around 500 nm can be seen in the spectra of the mixture. The results indicate that insufficient and excessive thiol-CD would unfavorable for the synthesis of nanoclusters. Thus, the ratio of HAuCl_4 to thiol-CD was chosen as 1:4 for the maximum fluorescence emission in the following experiment. The effect of NaOH concentration on the fluorescence intensity of produced thiol-CD-Au NCs is shown in Supporting materials, Fig. S5 C and D. By gradually increasing NaOH from 0.05 M to 0.3 M, the fluorescence intensity increases and reaches a maximum when NaOH was 0.15 M. Further increasing of NaOH led to fluorescence decreasing of thiol-CD-Au NCs. Therefore, 0.15 M of NaOH was selected to synthesize thiol-CD-Au NCs.

Temperature also plays a critical role in the synthesis of gold nanoclusters. We found that the fluorescent Au NCs only be produced at high temperatures. Fig. S6 shows the fluorescence intensity of the Au NCs synthesized at 70, 80 and 90 $^{\circ}\text{C}$ for a period. There is no fluorescence emission even reaction for 6 h at 70 $^{\circ}\text{C}$. If the temperature was increased to 80 and

90 °C, the fluorescence appeared after several hours. As shown in Electronic Supporting Material Fig. S7, the fluorescence appears after 3 h of reaction at 90 °C and reaches a maximum after 4 h. Further prolong of reaction gradually caused decreasing of fluorescence. Therefore, the synthesis of the Au NCs was carried out at 90 °C for 4 h for producing Au NCs with higher fluorescence intensity.

Selectivity and interference of nitrophenol isomers

As the steric hindrance of nitrophenol isomers for the hydrophobic cavity of β -CD follows the order 2-NP > 3-NP > 4-NP, the inclusion ability between β -CD and NP isomers follows the order 4-NP > 3-NP > 2-NP. For example, Zhang et al. [35] reported that the interaction of nitrophenol isomers and a fluorescent cyclodextrin capped CdTe quantum dots (CD-CdTe QDs) have different degrees of electron transfer fluorescence quenching. We also studied the fluorescence response between thiol-CD-Au NCs and nitrophenol isomers. As shown in Fig. 3a, b, the fluorescence of thiol-CD-Au NCs increased when mixed with 2-NP and 3-NP, however, quenched by the addition of 4-NP. We further measured the UV-vis absorption spectra of the mixture and found that the absorption feature of the three mixtures is different. As shown in Fig. 3c, the

mixture of 4-NP and Au NCs has a strong absorption peak at 430 nm, the mixture of 2-NP and Au NCs has a weak absorption peak at 442 nm, while 3-NP has no clear absorption in the visible light range. As shown in Fig. 3a, the fluorescence intensity decreased after mixing thiol-CD-Au NCs and 4-NP, and the fluorescence intensity was slightly enhanced when mixed with 3-NP and 2-NP, respectively, so we can identify 4-NP. In the UV-visible absorption spectrum (Fig. 3c), the UV-visible absorption value of the 2-NP mixture has a weak absorption peak at 442 nm, but the 3-NP has no absorption in the visible region, and we can identify 2-NP and 3-NP. Thus, after mixing three nitrophenols isomers with thiol-CD-Au NCs respectively, the three nitrophenols isomers can be easily distinguished by comparing their UV-visible absorption or fluorescence spectra. The interference of nitrophenol isomers and other similar compounds, such as 2-NP, 3-NP, phenol, 2,3-Dihydroxynaphthalene (DD), 1,3,5-Tris (4-aminophenyl) benzene (TAPB) and biphenyl diamine (DAB) on the determination of 4-NP was also studied. As shown in Electronic Supporting Material, Fig. S8, the result indicated that these chemicals could not obviously interfere.

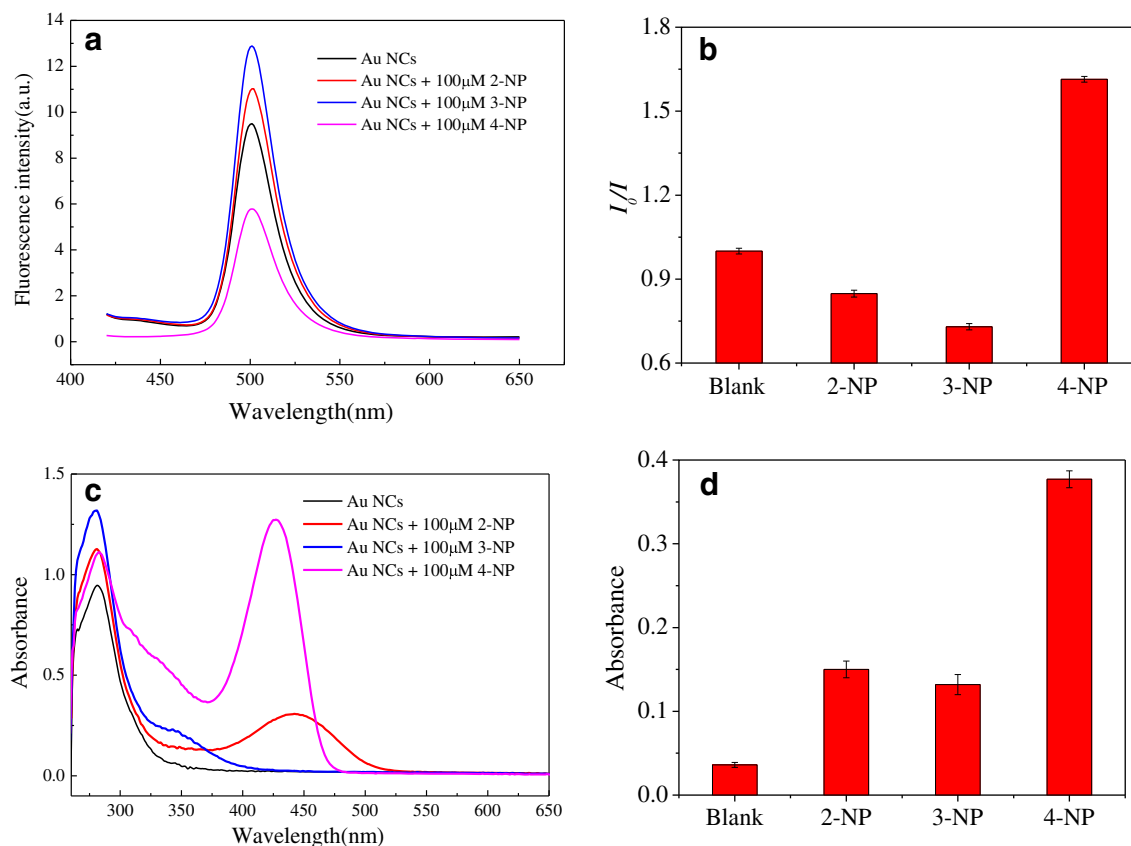


Fig. 3 Fluorescence spectra (a) and UV-vis absorption spectra (c) of thiol-CD-Au NCs in the presence of 100 μ M of 2-NP, 3-NP, 4-NP, and a comparison of fluorescence (b) and absorption (d) intensity change

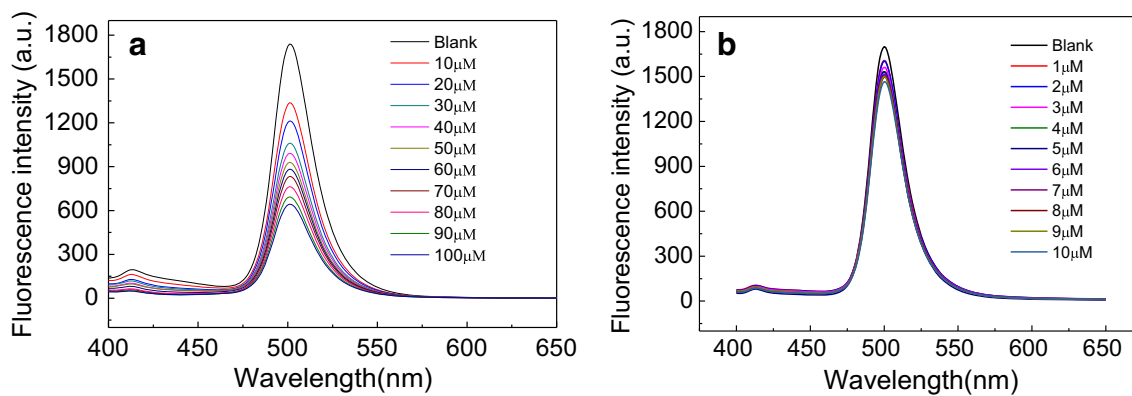
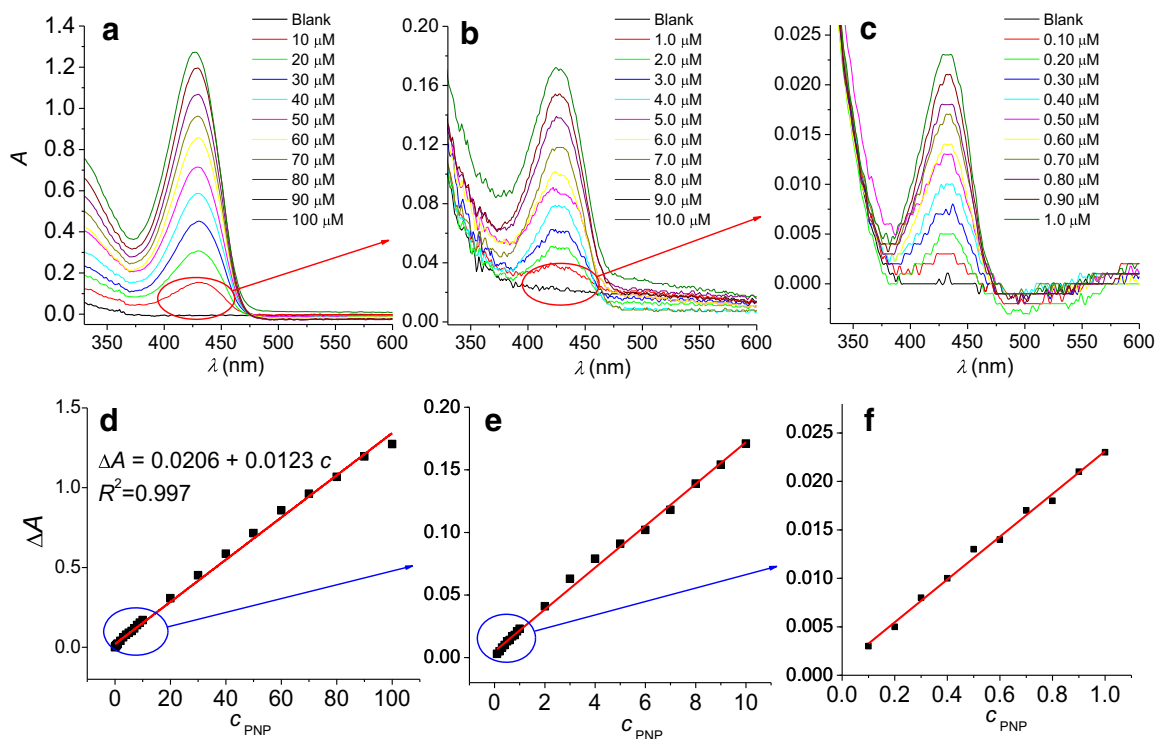


Fig. 4 Fluorescence spectra of the thiol-CD-Au NCs in the presence of different concentrations of 4-NP in the range from 10.0 to 100.0 μM (a) and 1.0 to 10.0 μM (b)



4-NP

added: 0 10.0 20.0 30.0 40.0 50.0 60.0 70.0 80.0 90.0 100.0

Fig. 5 UV-vis absorption of the thiol-CD-Au NCs in the presence of different concentrations of 4-NP in the range from 10.0 to 100.0 μM (a), 1.0 to 10.0 μM (b) and 0.1 to 1.0 μM (c). Linear relationship between

absorbance change and the concentration of 4-NP added (d-f) and the color pictures of thiol-CD-Au NCs after added 0–100 μM of 4-NP (g)

Application for 4-nitrophenol sensing

The fluorescence and absorption of thiol-CD-Au NCs toward 4-NP in the range from 0.1 to 100 μM were investigated using fluorescence and UV-vis absorption spectrometer. First, the fluorescence intensity of the Au NCs decreases gradually when the addition of 4-NP in the range from 10.0 to 100.0 μM . A lower concentration (less than 10 μM) of 4-NP can hardly quench the fluorescence of the Au NCs (Fig. 4). The Stern-Volmer plot is a straight line (Supplementary Material Fig. S9) that indicates the quenching is a static quenching. Second, the absorption spectra of the 4-NP and Au NCs mixture increases with the increasing of 4-NP. There is a characteristic absorption peak at 430 nm, and surprisingly, the absorbance is linearly increasing with the 4-NP in a wide concentration range from 0.1 to 100 μM (Fig. 5a-c). Although the high concentration of 4-NP (larger than 50 μM , supporting materials, Fig. S10) also has absorption in the same wavelength range (around 430 nm), the Au NCs can be used for sensing 4-NP at a lower concentration at 0.1 μM .

The absorption and fluorescence spectra of the 4-NP and thiol-CD-Au NCs indicate that the β -CD has excellent supramolecular recognition capability that formed inclusion complexes with 4-NP. As the UV-vis absorption spectrum of 4-NP and Au NCs mixture has overlap with the fluorescence excitation band (365 nm, Fig. 1a) of thiol-CD-Au NCs, the fluorescence quenching of thiol-CD-Au NCs was caused by inner filter effect (IFE) of the 4-NP/Au NCs complex. Thus, by measuring the absorption of the mixture of 4-NP-thiol-CD-Au NCs, it can establish an analytical method for selective and sensitive sensing of 4-NP. Compared with measuring the fluorescence changes of 4-NP-thiol-CD-Au NCs complex, the absorbance is stable and reliable.

Spectrometric and colorimetric determination of 4-nitrophenol

By using measuring the absorption spectra of 4-NP-Au NCs mixture, we found a good linear relationship between the absorbance changes at 430 nm (ΔA) and 4-NP concentration ($c_{4\text{-NP}}$) in the range from 0.1 to 100.0 μM . The standard regression equation is $\Delta A = 0.021 + 0.012 c_{4\text{-NP}}$, with a

Table 1 Quantitation of 4-NP in water samples

Sample	Add (μM)	Found (μM)	Recovery (%)	RSD ($n=3$, %)
1	0.0	N.D ^b	—	—
2	25.0	22.8	94.8	1.7
3	50.0	51.3	102.7	1.2

Water samples 1, 2, and 3 are from the Panlong River in Kunming. N.D^b means not detected

Table 2 Determination of PNP by other optical probes in recent papers

Probes	Linear range	LOD	Reference
Au@S-GQD	0–50 μM	0.0035 μM	[33]
Mn-doped ZnS QDs	0.1–40 μM	0.076 μM	[34]
CB/ β -CD	0.125–225.8 μM	0.04 μM	[36]
β -CD-CdTe QDs	20–100 μM	0.3 μM	[35]
Si4Pic ⁺ Cl ⁻ -Au NPs	0.1–1.5 μM	0.046 μM	[32]
Thiol-CD-Au NCs	0.1–100 μM	0.09 μM	This work

corresponding coefficient of determination of 0.997 and detection limits of 0.087 μM (Fig. 5d). The relationship is very wide and is linear at lower 4-NP concentration (Fig. 5e, f). Furthermore, a colorimetric assay was processed directly using the 4-NP-Au NCs mixture in glass tubes to detect a different amount of 4-NP at higher concentration. Figure 5g shows the picture of the 4-NP-Au NCs solution after interacting with ten different concentrations of 4-NP in the range from 10.0 to 100.0 μM . The color of mixtures gets changed from colorless to yellow with increasing of 4-NP. By comparing with the standard colorimetric picture, we can probably discriminate the concentration of 4-NP visually.

To further investigate the practicality and accuracy in a practical sample, we collected samples from a local river to test the reliability of the method by the standardized addition method. As shown in Table 1, the results indicated that the method had a recovery from 94.8% to 102.7% for the detection of 4-NP at higher concentration. However, as the background absorption in the ultraviolet region of river water, it is a pity that it is very hard to detect 4-NP with a concentration lower than 1 μM in the river water sample. We also compared the analytical parameters with published papers that separation and detection of nitrophenols using similar methods (Table 2). The analytical parameters in this paper are comparable with or even better than reported analytical methods. As the 4-NP can be easily determined using thiol-CD-Au NCs by both UV-visible absorption and fluorescence methods, we believe that the thiol-CD-Au NCs Probe has the potential for further applications in other analytical fields.

Conclusion

We utilized a rapid hydrothermal method for synthesis a new type of green emission fluorescent gold nanoclusters by introducing thiol-cyclodextrin as a template. The thiol- β -cyclodextrin Au nanoclusters (thiol-CD-Au NCs) has green fluorescence emission around 502 nm with a narrow bandwidth near 30 nm. We studied the fluorescence property of the nanoclusters and discussed the mechanism of the nanocluster formation. The hydroxyl in the β -cyclodextrin reduced the Au⁴⁺ to Au⁰ and the produced Au NCs was

stabilized by the thiol- β -cyclodextrin. The nanoclusters were successfully used for the discrimination of nitrophenol isomers. 4-nitrophenol in the range from 0.1 to 100.0 μM was selectively detected using a common spectrophotometer or distinguished visually. However, for practical sample detection, as the background absorption in the ultraviolet region, it is very hard to detect 4-NP with a concentration lower than 1 μM in the river water sample. For the synthesis of nanoclusters, we believed the hydrothermal method can be used for more noble metal nanoclusters preparation and the green-emission Au NCs can be used for more analytical applications, such as Förster resonance energy transfer.

Acknowledgements This work was financially supported by the National Natural Science Foundation of China (No. 21565030), Program for Excellent Young Talents of Yunnan University and National Demonstration Center for Experimental Chemistry and Chemical Engineering Education (Yunnan University).

Compliance with ethical standards

Conflict of interest The authors declare that they have no conflict of interest.

References

- Jin R (2010) Quantum sized, thiolate-protected gold nanoclusters. *Nanoscale* 2(3):343–362. <https://doi.org/10.1039/b9nr00160c>
- Zeng C, Chen Y, Li G, Jin R (2014) Synthesis of a Au44(SR)28 nanocluster: structure prediction and evolution from Au28(SR)20, Au36(SR)24 to Au44(SR)28. *Chem Commun* 50(1):55–57. <https://doi.org/10.1039/C3CC47089J>
- Yu Y, Luo Z, Chevrier DM, Leong DT, Zhang P, D-e J, Xie J (2014) Identification of a highly luminescent Au22(SG)18 Nanocluster. *J Am Chem Soc* 136:1246–1249. <https://doi.org/10.1021/ja411643u>
- Jin R, Zeng C, Zhou M, Chen Y (2016) Atomically precise colloidal metal nanoclusters and nanoparticles: fundamentals and opportunities. *Chem Rev* 116(18):10346–10413. <https://doi.org/10.1021/acs.chemrev.5b00703>
- Peng H, Jian M, Deng H, Wang W, Huang Z, Huang K, Liu A, Chen W (2017) Valence states effect on Electrogenerated Chemiluminescence of gold nanocluster. *ACS Appl Mater Interfaces* 9(17):14929–14934. <https://doi.org/10.1021/acsami.7b02446>
- Hu X, Zheng Y, Zhou J, Fang D, Jiang H, Wang X (2018) Silver-assisted thiolate ligand exchange induced photoluminescent boost of gold nanoclusters for selective imaging of intracellular glutathione. *Chem Mater* 30(6):1947–1955. <https://doi.org/10.1021/acs.chemmater.7b04926>
- Weng B, Lu K-Q, Tang Z, Chen HM, Xu Y-J (2018) Stabilizing ultrasmall Au clusters for enhanced photoredox catalysis. *Nat Commun* 9(1):1543. <https://doi.org/10.1038/s41467-018-04020-2>
- Dou Y, Yang X (2013) Novel high-sensitive fluorescent detection of deoxyribonuclease I based on DNA-templated gold/silver nanoclusters. *Anal Chim Acta* 784(0):53–58. <https://doi.org/10.1016/j.aca.2013.04.038>
- Liang S, Kuang Y, Ma F, Chen S, Long Y (2016) A sensitive spectrofluorometric method for detection of berberine hydrochloride using Ag nanoclusters directed by natural fish sperm DNA. *Biosens Bioelectron* 85:758–763. <https://doi.org/10.1016/j.bios.2016.05.070>
- Xie JP, Zheng YG, Ying JY (2010) Highly selective and ultrasensitive detection of Hg²⁺ based on fluorescence quenching of Au nanoclusters by Hg²⁺-Au⁺ interactions. *Chem Commun* 46(6):961–963. <https://doi.org/10.1039/b920748a>
- Chen W, Tu X, Guo X (2009) Fluorescent gold nanoparticles-based fluorescence sensor for Cu²⁺ ions. *Chem Commun*:1736–1738. <https://doi.org/10.1039/b820145e>
- Bai X, Xu S, Wang L (2018) Full-range pH stable Au-clusters in nanogel for confinement-enhanced emission and improved sulfide sensing in living cells. *Anal Chem* 90:3270–3275. <https://doi.org/10.1021/acs.analchem.7b04785>
- Li Z, Liu R, Xing G, Wang T, Liu S (2017) A novel fluorometric and colorimetric sensor for iodide determination using DNA-templated gold/silver nanoclusters. *Biosens Bioelectron* 96:44–48. <https://doi.org/10.1016/j.bios.2017.01.005>
- Zhang L, Song W, Liang RP, Qiu JD (2016) Simultaneous determination of protein kinase a and casein kinase II by dual-color peptide biomimetic metal Nanoclusters. *Anal Chem* 88(23):11460–11467. <https://doi.org/10.1021/acs.analchem.6b02522>
- Duan Y, Duan R, Liu R, Guan M, Chen W, Ma J, Chen M, Du B, Zhang Q (2018) Chitosan-stabilized self-assembled fluorescent gold Nanoclusters for cell imaging and biodistribution in vivo. *ACS Biomater Sci Eng* 4:1055–1063. <https://doi.org/10.1021/acsbiomaterials.7b00975>
- Zhang P, Lan J, Wang Y, Xiong ZH, Huang CZ (2015) Luminescent golden silk and fabric through in situ chemically coating pristine-silk with gold nanoclusters. *Biomaterials* 36:26–32. <https://doi.org/10.1016/j.biomaterials.2014.08.026>
- Gao Y, Shao N, Zeng XC (2008) Ab initio study of thiolate-protected Au102 nanocluster. *ACS Nano* 2(7):1497–1503. <https://doi.org/10.1021/nn800268w>
- Luo QJ, Li ZG, Lai JH, Li FQ, Qiu P, Wang XL (2017) An on-off-on gold nanocluster-based fluorescent probe for sensitive detection of organophosphorus pesticides. *RSC Adv* 7(87):55199–55205. <https://doi.org/10.1039/c7ra11835j>
- Jiang H, Su X, Zhang Y, Zhou J, Fang D, Wang X (2016) Unexpected thiols triggering photoluminescent enhancement of cytidine stabilized Au nanoclusters for sensitive assays of glutathione reductase and its inhibitors screening. *Anal Chem* 88(9):4766–4771. <https://doi.org/10.1021/acs.analchem.6b00112>
- Bain D, Maity S, Paramanik B, Patra A (2018) Core-size dependent fluorescent gold nanoclusters and ultrasensitive detection of Pb²⁺ ion. *ACS Sustain Chem Eng* 6(2):2334–2343. <https://doi.org/10.1021/acssuschemeng.7b03794>
- Kawasaki H, Hamaguchi K, Osaka I, Arakawa R (2011) pH-dependent synthesis of pepsin-mediated gold nanoclusters with blue green and red fluorescent emission. *Adv Funct Mater* 21(18):3508–3515. <https://doi.org/10.1002/adfm.201100886>
- Guo Y, Guo S, Ren J, Zhai Y, Dong S, Wang E (2010) Cyclodextrin functionalized graphene nanosheets with high supramolecular recognition capability: synthesis and host-guest inclusion for enhanced electrochemical performance. *ACS Nano* 4(7):4001–4010. <https://doi.org/10.1021/nn100939n>
- Chen G, Jiang M (2011) Cyclodextrin-based inclusion complexation bridging supramolecular chemistry and macromolecular self-assembly. *Chem Soc Rev* 40(5):2254–2266. <https://doi.org/10.1039/c0cs00153h>
- Cao S, An X (2018) In-situ synthesis of fluorescent Ag clusters using β -cyclodextrins cavity as templates. *Mater Lett* 216:170–172. <https://doi.org/10.1016/j.matlet.2017.12.086>
- Halawa MI, Wu F, Fereja TH, Lou B, Xu G (2018) One-pot green synthesis of supramolecular β -cyclodextrin functionalized gold nanoclusters and their application for highly selective and sensitive

- fluorescent detection of dopamine. *Sensors Actuators B Chem* 254: 1017–1024. <https://doi.org/10.1016/j.snb.2017.07.201>
26. Wang Y, Guo H, Zhang Y, Tai F, Wang Y, Dong Q, Nie Y, Zhao Q, Wong W-Y (2018) Achieving highly water-soluble and luminescent gold nanoclusters modified by β -cyclodextrin as multifunctional nanoprobe for biological applications. *Dyes Pigments* 157: 359–368. <https://doi.org/10.1016/j.dyepig.2018.05.015>
 27. Gupta VK, Atar N, Yola ML, Ustundag Z, Uzun L (2014) A novel magnetic Fe@Au core-shell nanoparticles anchored graphene oxide recyclable nanocatalyst for the reduction of nitrophenol compounds. *Water Res* 48:210–217. <https://doi.org/10.1016/j.watres.2013.09.027>
 28. Xu X, Liu Z, Zhang X, Duan S, Xu S, Zhou C (2011) β -Cyclodextrin functionalized mesoporous silica for electrochemical selective sensor: simultaneous determination of nitrophenol isomers. *Electrochim Acta* 58:142–149. <https://doi.org/10.1016/j.electacta.2011.09.015>
 29. Oturan MA, Peiroten J, Chartrin P, Acher AJ (2000) Complete destruction of p-nitrophenol in aqueous medium by Electro-Fenton method. *Environ Sci Technol* 34(16):3474–3479. <https://doi.org/10.1021/es990901b>
 30. Manera M, Miro M, Estela JM, Cerda V (2007) Multi-syringe flow injection solid-phase extraction system for on-line simultaneous spectrophotometric determination of nitro-substituted phenol isomers. *Anal Chim Acta* 582(1):41–49. <https://doi.org/10.1016/j.aca.2006.08.063>
 31. Yang L, Fan S, Deng G, Li Y, Ran X, Zhao H, Li CP (2015) Bridged beta-cyclodextrin-functionalized MWCNT with higher supramolecular recognition capability: the simultaneous electrochemical determination of three phenols. *Biosens Bioelectron* 68:617–625. <https://doi.org/10.1016/j.bios.2015.01.059>
 32. Silva PS, Gasparini BC, Magosso HA, Spinelli A (2014) Gold nanoparticles hosted in a water-soluble silsesquioxane polymer applied as a catalytic material onto an electrochemical sensor for detection of nitrophenol isomers. *J Hazard Mater* 273:70–77. <https://doi.org/10.1016/j.jhazmat.2014.03.032>
 33. Anh NTN, R-a D (2018) One-step synthesis of size-tunable gold@sulfur-doped graphene quantum dot nanocomposites for highly selective and sensitive detection of Nanomolar 4-Nitrophenol in aqueous solutions with complex matrix. *ACS Appl Nano Mater* 1(5):2153–2163. <https://doi.org/10.1021/acsnanm.8b00210>
 34. Liu J, Chen H, Lin Z, Lin J-M (2010) Preparation of surface imprinting polymer capped Mn-doped ZnS quantum dots and their application for chemiluminescence detection of 4-Nitrophenol in tap water. *Anal Chem* 82(17):7380–7386. <https://doi.org/10.1021/ac101510b>
 35. Zhang Z, Zhou J, Liu Y, Tang J, Tang W (2015) Cyclodextrin capped CdTe quantum dots as versatile fluorescence sensors for nitrophenol isomers. *Nanoscale* 7(46):19540–19546. <https://doi.org/10.1039/C5NR06073G>
 36. Kubendhiran S, Sakthivel R, Chen S-M, Mutharani B, Chen T-W (2018) Innovative strategy based on a novel carbon-black- β -cyclodextrin nanocomposite for the simultaneous determination of the anticancer drug flutamide and the environmental pollutant 4-Nitrophenol. *Anal Chem* 90(10):6283–6291. <https://doi.org/10.1021/acs.analchem.8b00989>
 37. Fischer J, Berek J, Wang J (2006) Separation and detection of nitrophenols at capillary electrophoresis microchips with amperometric detection. *Electroanalysis* 18(2):195–199. <https://doi.org/10.1002/elan.200503393>
 38. Xie J, Zheng Y, Ying JY (2009) Protein-directed synthesis of highly fluorescent gold nanoclusters. *J Am Chem Soc* 131(3):888–889. <https://doi.org/10.1021/ja806804u>
 39. Chaudhari K, Xavier PL, Pradeep T (2011) Understanding the evolution of luminescent gold quantum clusters in protein templates. *ACS Nano* 5(11):8816–8827. <https://doi.org/10.1021/nn202901a>
 40. Wu ZK, Jin RC (2010) On the Ligand's role in the fluorescence of gold nanoclusters. *Nano Lett* 10(7):2568–2573. <https://doi.org/10.1021/nl101225f>

Publisher's note Springer Nature remains neutral with regard to jurisdictional claims in published maps and institutional affiliations.